Spectral magnetization ratchets with discrete-time quantum walks

A. Mallick,[1,*] M. V. Fistul,[1,2] P. Kaczynska,[1,3] and S. Flach[1]

[1]*Center for Theoretical Physics of Complex Systems, Institute for Basic Science (IBS), Daejeon 34126, Republic of Korea*

[2]*National University of Science and Technology "MISIS", Russian Quantum Center, Moscow 119049, Russia*

[3]*Faculty of Physics, University of Warsaw, Warsaw 02-093, Poland*

(Received 13 January 2020; accepted 25 February 2020; published 31 March 2020)

We predict and theoretically study in detail the ratchet effect for the spectral magnetization of *periodic* discrete-time quantum walks (DTQWs)—a repetition of a sequence of m different DTQWs. These generalized DTQWs are achieved by varying the corresponding coin operator parameters periodically with discrete time. We consider periods $m = 1, 2$, and 3. The dynamics of m-periodic DTQWs is characterized by a two-band dispersion relation $\omega_{\pm}^{(m)}(k)$, where k is the wave vector. We identify a generalized parity symmetry of m-periodic DTQWs. The symmetry can be broken for $m = 2$ and 3 by proper choices of the coin operator parameters. The obtained symmetry breaking results in a ratchet effect, i.e., the appearance of a nonzero spectral magnetization $M_s(\omega)$. This ratchet effect can be observed in the framework of continuous quantum measurements of a time-dependent correlation function of periodic DTQWs.

DOI: 10.1103/PhysRevA.101.032119

I. INTRODUCTION

Dynamical properties of particles and waves in spatially periodic structures that are driven by external time-dependent forces manifestly depend on the space-time symmetries of the underlying equations of motion. A systematic analysis of these symmetries uncovers the conditions necessary for their violation and the appearance of the ratchet phenomenon to, e.g., explain rectification of currents, polarizations, magnetizations, and vorticity [1–4]. Such phenomena have been predicted and studied in detail in various Hamiltonian and dissipative systems, for single-particle [5] and for many-body interacting [6] systems. Ratchets have been observed in various solid-state [7], optical [8], and chemical and biological [2] systems.

Classical ratchet experimental platforms are modeled with a set of coupled nonlinear differential equations whose parameters vary in space and time. The ratchet effect results from broken spatiotemporal symmetries of the differential equations. Spatiotemporal symmetries typically involve discrete shift and parity operations [4].

The quantum ratchet concept was predicted theoretically [9–11] and successfully implemented for a variety of different quantum systems platforms [12–14]. Quantum ratchets are typically described by quantum Hamiltonian systems which are periodically driven in time. The main body of studies was devoted to rectifying charge currents. For driven and damped spins an incoherent ratchet effect realized in the form of a nonzero static magnetization was reported in Refs. [15,16]. Spectral magnetization ratchets, i.e., frequency-selective magnetization ratchets for coherent nondissipative quantum spin systems, including discrete-time quantum walk platforms, are an area ripe for investigation.

To address the coherent quantum spin ratchet dynamics, we use the platform of discrete-time quantum walks (DTQWs) [17]. A DTQW is a spatiotemporal unitary map developed for quantum computing [18,19], which is obtained from a repeating sequence of coin and shift operators acting on a two-level (spin-1/2) system network. Recently such platforms turned into a playground to study various interesting physical phenomena, e.g., single-particle and many-body Anderson localization [20–22], topological phenomena [23–26], propagating solitons [27], relativistic Dirac particle systems [28–30], etc. DTQWs have been experimentally implemented using ion traps, photonic crystals, NMR [31], cavity QED [32], etc. DTQW ratchets [33–35] were introduced for directed currents.

In order to obtain the spectral magnetization effect with DTQWs we introduce their generalization—m-periodic DTQWs—a repetition of a sequence of m different DTQWs (see, e.g., Refs. [36–39]). These generalized DTQWs are achieved by varying the corresponding coin operator parameters periodically as functions of the discrete time. We identify various symmetries of m-periodic DTQWs and outline ways to break them for $m = 2$ and 3. This ratchet effect can be observed in the framework of continuous quantum measurements of a time-dependent correlation function of periodic DTQWs.

The paper is organized as follows. We first introduce the model and dynamic equations for m-periodic DTQWs. We proceed with defining dispersion relations, eigenvectors, and magnetization properties. We continue to define the generalized parity symmetry. For $m = 1$, 2, and 3 we analyze the conditions under which the generalized parity is broken, derive the symmetry-breaking conditions, and obtain a spectral magnetization ratchet for $m = 2$ and 3. Finally, we discuss observation methods and conclude.

*marindam@ibs.re.kr

II. *m*-PERIODIC DISCRETE-TIME QUANTUM WALKS

We consider a single-particle m-periodic DTQW which is defined on a lattice of N sites. The quantum-mechanical dynamics of arbitrary DTQW is characterized by two-component wave functions $|\psi(n,t)\rangle = [\psi_+(n,t),\ \psi_-(n,t)]^T$ which depend on both site n and discrete time t. The discrete-time-dependent probability amplitude for the whole system is characterized by the state $|\psi(t)\rangle = \sum_{n=1}^{N} |n\rangle \otimes |\psi(n,t)\rangle$. The m-periodic dynamics of such wave functions is determined by coin operators $\hat{C}_\ell$, with the temporal index ℓ varying from 1 to m, and a shift operator, $\hat{S}$, acting on the state as follows:

$$|\psi(t+\ell)\rangle = \hat{S}\cdot\hat{C}_\ell\ |\psi(t+\ell-1)\rangle\,, \quad \ell = 1,\ldots,m. \tag{1}$$

We consider site-independent coin operators $\hat{C}_\ell$:

$$\hat{C}_\ell = \mathbb{1}\otimes e^{i\varphi_\ell}\begin{pmatrix} e^{i\varphi_{1,\ell}}\cos\theta_\ell & e^{i\varphi_{2,\ell}}\sin\theta_\ell \\ -e^{-i\varphi_{2,\ell}}\sin\theta_\ell & e^{-i\varphi_{1,\ell}}\cos\theta_\ell \end{pmatrix}, \tag{2}$$

where $\mathbb{1}$ is the identity operator on position space, i.e., with rank N for a total number of N sites. The DTQW dynamics at each time t is determined by four angles: φ, φ_1, φ_2, and θ. These angles can be related to the action of a potential energy, an external synthetic magnetic flux, an internal synthetic magnetic flux, and a kinetic energy, respectively [20]. As outlined below, the potential energy angle φ turns irrelevant, and we always set it to zero: $\varphi = 0$. The shift operator couples neighboring sites by transferring the $\psi_+(n,t)$ components one step to the right and the $\psi_-(n,t)$ components to the left:

$$\hat{S} = \sum_n |n\rangle\langle n+1|\otimes|-\rangle\langle-| \ +\ |n\rangle\langle n-1|\otimes|+\rangle\langle+|\,. \tag{3}$$

We then arrive at the generalized evolution operator of m-periodic DTQWs:

$$\hat{U}^{(m)} = \prod_{l=1}^{m}\hat{U}_\ell = \prod_{l=1}^{m}\hat{S}\cdot\hat{C}_\ell. \tag{4}$$

The schematic of the DTQW evolution is presented in Fig. 1.

Translational invariance of the evolution operator $\hat{U}_\ell = \hat{S}\cdot\hat{C}_\ell$ allows one to apply Bloch's theorem and to expand the wave function in the plane-wave basis as $|\psi(n,t)\rangle = \frac{1}{\sqrt{N}}\sum_k e^{ikn}|\psi(k,t)\rangle$, where $|\psi(k,t)\rangle = [\psi_+(k,t),\ \psi_-(k,t)]^T$ is the two-component wave function in momentum space. The dynamics of an m-periodic DTQW in k-space follows as

$$|\psi(k,t+m)\rangle = \prod_{\ell=1}^{m}\hat{U}_\ell(k)\,|\psi(k,t)\rangle\,. \tag{5}$$

The evolution operator for a single m-period can be written as $\hat{U}^{(m)} = \sum_k |k\rangle\langle k|\otimes\hat{U}^{(m)}(k) = \sum_k |k\rangle\langle k|\otimes\prod_{\ell=1}^{m}\hat{U}_\ell(k)$, where

$$\hat{U}_\ell(k) = e^{i\varphi_\ell}\begin{pmatrix} e^{i\varphi_{1,\ell}-ik}\cos\theta_\ell & e^{i\varphi_{2,\ell}-ik}\sin\theta_\ell \\ -e^{-i\varphi_{2,\ell}+ik}\sin\theta_\ell & e^{-i\varphi_{1,\ell}+ik}\cos\theta_\ell \end{pmatrix}. \tag{6}$$

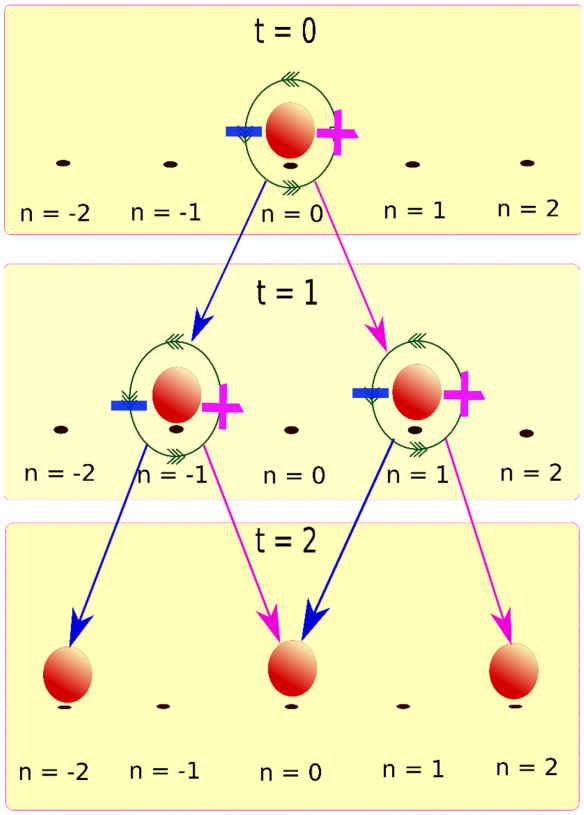

FIG. 1. Schematic representation of the 1-periodic DTQW. The lattice sites n are denoted by black dots, and time flows from top to bottom following the arrows. The DTQW wave function $|\psi(n,t)\rangle$ is initialized at $t = 0$ and site $n = 0$ and evolves as denoted by straight arrows. The "±" signs indicate two spin-components [magenta (light gray) and blue (gray)]. The double-arrow-decorated circles indicate coin operations which rotate the spin components at each site. The straight arrows indicate the shift operations with the "+" component shifted along the magenta (light gray) arrow to the down right and the "−" component shifted along the blue (gray) arrow to the down left.

III. DISPERSION RELATIONS AND EIGENVECTORS

The solution of Eq. (5) is written as $|\psi(k,t)\rangle = e^{-i\omega^{(m)}t}\,|\psi(k,\omega^{(m)})\rangle$, where $|\psi(k,\omega^{(m)})\rangle = [\psi_+(k,\omega^{(m)}),\ \psi_-(k,\omega^{(m)})]^T$ is the corresponding two-component wave function in momentum and frequency space. The frequency $\omega^{(m)}$ is a function of the momentum k and can take two values for a fixed value of k, i.e., $\omega_\pm^{(m)}(k)$. This follows directly from having two levels (degrees of freedom) per lattice site (unit cell), which dictates a band structure with two bands. From Eqs. (5) and (6) it follows that nonzero values of the angles φ_ℓ result in a shift of $\omega_\pm^{(m)}$ only. This is similar to a potential which is constant in space and only shifts the energy of a quantum system. Therefore we set $\varphi_\ell = 0$ for all l.

The evolution operator

$$\hat{U}^{(m)}(k) = \prod_{\ell=1}^{m}\hat{U}_\ell(k) = \begin{pmatrix} u_{11}^{(m)} & u_{12}^{(m)} \\ -\left[u_{12}^{(m)}\right]^\star & \left[u_{11}^{(m)}\right]^\star \end{pmatrix} \tag{7}$$

is a unitary matrix, whose eigenvalues yield the dispersion relation of m-periodic DTQWs:

$$\omega_{\pm}^{(m)}(k) = \pm\frac{1}{m}\arccos\left(\mathrm{Re}\left[u_{11}^{(m)}(k)\right]\right). \tag{8}$$

For each value of the wave number k we find two frequencies with opposite values. Thus the band structure of any m-periodic DTQW is given by two bands which have symmetry related by Eq. (8). Because of Bloch's theorem, the matrix elements $u_{\alpha\beta}^{(m)}$ for all α and β in Eq. (7) are periodic functions of k. Hence $\omega_{\pm}^{(m)}(k)$ is also a periodic function of k. The corresponding eigenvectors are given by $|k\rangle \otimes |\psi(k, \omega_{\pm}^{(m)})\rangle$, with the spinor part

$$|\psi(k, \omega_{\pm}^{(m)})\rangle = \frac{\left[iu_{12}^{(m)},\ \mathrm{Im}\left[u_{11}^{(m)}\right] + \sin[m\omega_{\pm}^{(m)}]\right]^T}{\sqrt{\left|u_{12}^{(m)}\right|^2 + \left|\mathrm{Im}\left[u_{11}^{(m)}\right] + \sin[m\omega_{\pm}^{(m)}]\right|^2}}. \tag{9}$$

IV. MAGNETIZATION

The magnetization of an eigenstate measures the population imbalance between the upper and lower levels. It is obtained from the expectation value of the magnetization operator $\hat{M} = \mathbb{1} \otimes \hat{\sigma}_3$ as

$$\begin{aligned} M_{\pm}(k) &= \langle k|\mathbb{1}|k\rangle\, \langle\psi(k, \omega_{\pm}^{(m)})|\hat{\sigma}_3|\psi(k, \omega_{\pm}^{(m)})\rangle \\ &= |\psi_+(k, \omega_{\pm}^{(m)})|^2 - |\psi_-(k, \omega_{\pm}^{(m)})|^2. \end{aligned} \tag{10}$$

With Eqs. (9) and (10) it follows that

$$M_{\pm}(k) = \frac{-\mathrm{Im}\left[u_{11}^{(m)}(k)\right]}{\sin[m\omega_{\pm}^{(m)}(k)]} = \mp\frac{\mathrm{Im}\left[u_{11}^{(m)}(k)\right]}{\sqrt{1 - \left\{\mathrm{Re}\left[u_{11}^{(m)}(k)\right]\right\}^2}}. \tag{11}$$

Note that $\pm$ in $M_{\pm}(k)$ refers respectively to the upper and lower branch of the two-band dispersion relation.

The above result (11) is quite remarkable and can be used for a number of conclusions. The magnetization of an eigenstate is entirely defined by the matrix element $u_{11}^{(m)}(k)$ of the evolution operator $\hat{U}^{(m)}(k)$, cf. Eqs. (7) and (8). It follows that the upper- and lower-branch magnetizations are opposite to each other: $M_+(k) = -M_-(k)$. Exciting a monochromatic (single wavelength) mix of states with one value of k and equal weights of eigenstates yields zero monochromatic magnetization,

$$M_k = M_+(k) + M_-(k) = 0, \tag{12}$$

for any m-periodic DTQW. Thus also the total magnetization M_{tot}—the sum over the magnetization values for all eigenstates (with equal weight)—vanishes pairwise for each k and is exactly zero for any m-periodic DTQW:

$$M_{\mathrm{tot}} = \sum_k M_k = 0. \tag{13}$$

At variance to the above, the spectral magnetization $M_s(\omega)$ measures the average magnetization of all eigenstates with $\omega_{\pm}(k_l) = \omega$. Different eigenstates with identical frequencies can be excited using spectroscopic methods, as we show below. Due to the fact that $\mathrm{Re}[u_{11}(k)]$ and consequently $\omega_{\pm}(k)$ are periodic functions of k, the spectral magnetization will average over a discrete set of eigenstates counted by the integer l:

$$M_s(\omega) = \sum_{k_l} M_{\pm}(k_l), \quad \omega = \omega_{\pm}(k_l). \tag{14}$$

For a fixed value of ω, the denominator in Eq. (11) is invariant for all allowed values of k_l. Further, since $\omega_{\pm}(k)$ is real and a periodic function in k, the set $\{|k_l\rangle\}$ contains an even number of states. The rest of this work is devoted to answering the following question: under which conditions will a generalized parity symmetry hold such that the set $\{|k_l\rangle\}$ will have symmetry-related pairs of states for which the magnetization vanishes pairwise? The breaking of that generalized parity symmetry will then lead to a nonzero spectral magnetization. We coin this effect *spectral magnetization ratchet*.

V. GENERALIZED PARITY SYMMETRY

The spectral magnetization ratchet requires the breaking of the *generalized parity symmetry*. If the ratchet effect is absent, the m-periodic DTQW is invariant under the action of the generalized parity symmetry operation:

$$\hat{U}^{(m)} = (\mathcal{P} \otimes \mathcal{G}) \cdot \hat{U}^{(m)} \cdot (\mathcal{P} \otimes \mathcal{G})^{\dagger}, \tag{15}$$

where $\mathcal{P}$ is an operator inducing reflection in momentum space around some wave number K, and $\mathcal{G}$ is an operator inducing spin flips with an additional phase shift G:

$$\begin{aligned} \mathcal{P} &= \sum_k |2K - k\rangle\, \langle k| = \sum_x e^{-2iKx}\, |-x\rangle\, \langle x|\,, \\ \mathcal{G} &= \begin{pmatrix} 0 & -e^{iG} \\ 1 & 0 \end{pmatrix}. \end{aligned} \tag{16}$$

If existing, the values of K and G will depend on the particular parameters of the m-periodic DTQW—hence the term *generalized* parity. In the presence of that symmetry, for each eigenstate $|k\rangle \otimes |\psi(k, \omega_{\pm}^{(m)})\rangle$ there exists another eigenstate, $|2K - k\rangle \otimes |\psi(2K - k, \omega_{\pm}^{(m)})\rangle$, such that

$$\mathcal{G}|\psi(k, \omega_{\pm}^{(m)})\rangle = |\psi(2K - k, \omega_{\pm}^{(m)})\rangle, \tag{17}$$

i.e., both states share the same eigenfrequency $\omega_{\pm}^{(m)}$. In terms of the matrix elements of the evolution operator $\hat{U}^{(m)}$, this symmetry implies

$$u_{11}^{(m)}(2K - k) = \left[u_{11}^{(m)}(k)\right]^*, \tag{18}$$

$$u_{12}^{(m)}(2K - k) = e^{iG}\left[u_{12}^{(m)}(k)\right]^*. \tag{19}$$

The consequence of Eq. (17) is $M_s(\omega) = 0$. Indeed, the parity operator $\mathcal{G}$ swaps the spin components and therefore reverts the sign of the magnetization (11), which then leads to opposite magnetizations of $|\psi(k, \omega_{\pm}^{(m)})\rangle$ and $|\psi(2K - k, \omega_{\pm}^{(m)})\rangle$. In operator form the generalized parity symmetry, Eqs. (17)–(19), can be expressed as

$$(\mathcal{P} \otimes \mathcal{G}) \cdot \hat{M} \cdot (\mathcal{P} \otimes \mathcal{G})^{\dagger} = -\hat{M}. \tag{20}$$

In order to realize the spectral magnetization ratchet effect, i.e., $M_s(\omega) \neq 0$, one needs to *break* the generalized parity symmetry, Eqs. (17)–(20). In the next section we explicitly

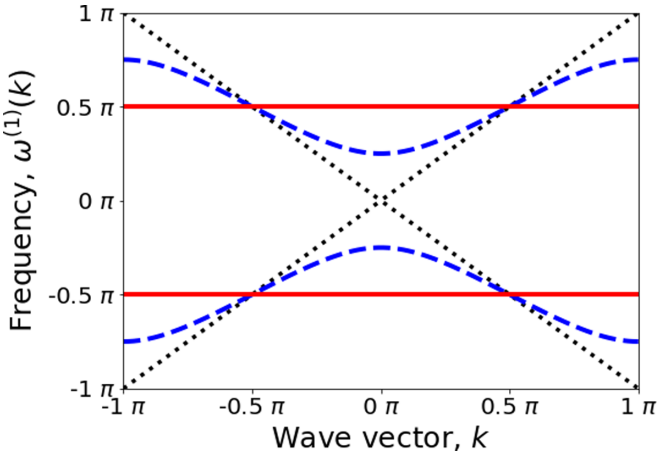

FIG. 2. Dispersion relation $\omega_{\pm}(k)$ for $m = 1$. $\theta_1 = 0$ (black dotted lines), $\theta_1 = \pi/4$ (blue dashed lines), and $\theta_1 = \pi/2$ (red solid lines). Other parameters: $\varphi_{1,1} = \varphi_{2,1} = 0$.

show how to break the generalized parity symmetry and realize the ratchet effect for $m = 2$-periodic and $m = 3$-periodic DTQWs.

VI. THE SPECTRAL MAGNETIZATION RATCHET

A. $m = 1$

For $m = 1$, the dispersion relation is written explicitly as [20]

$$\omega_{\pm}^{(1)}(k) = \pm \arccos[\cos(\theta_1)\cos(k - \varphi_{1,1})]. \tag{21}$$

Typical two-band dispersion relations $\omega_{\pm}^{(1)}(k)$ for various values of θ_1 are shown in Fig. 2.

With Eq. (6) we find

$$u_{11}^{(1)} = e^{i(\varphi_{1,1}-k)}\cos\theta_1, \tag{22}$$

$$u_{12}^{(1)} = e^{i(\varphi_{2,1}-k)}\sin\theta_1. \tag{23}$$

It follows that the generalized parity symmetry relations (18) and (19) are satisfied for all coin parameters of the DTQW with the notations $K = \varphi_{1,1}$ and $G = 2(\varphi_{2,1} - \varphi_{1,1})$. Therefore the spectral magnetization $M_s(\omega) = 0$, and a single-period DTQW always possesses generalized parity symmetry. This happens remarkably despite the action of both nonzero external and internal magnetic fluxes $\varphi_{1,1}$ and $\varphi_{2,1}$.

For the 1-periodic DTQW all eigenstates are doubly degenerated, and using Eqs. (21) and (11) we obtain

$$M_+(k) = \frac{\cos(\theta_1)\sin(k - \varphi_{1,1})}{\sqrt{1 - \cos^2(\theta_1)\cos^2(k - \varphi_{1,1})}}. \tag{24}$$

In line with the above symmetry analysis the spectral magnetization vanishes, as is also observed from the loop symmetry in Fig. 3.

B. $m = 2$

For $m = 2$ we calculate the product of two operators, $\hat{U}_1(k)$ and $\hat{U}_2(k)$, and find

$$u_{11}^{(2)} = \cos(\theta_1)\cos(\theta_2)e^{-i(2k-\varphi_{1,1}-\varphi_{1,2})} - \sin(\theta_1)\sin(\theta_2)e^{i(\varphi_{2,2}-\varphi_{2,1})},$$

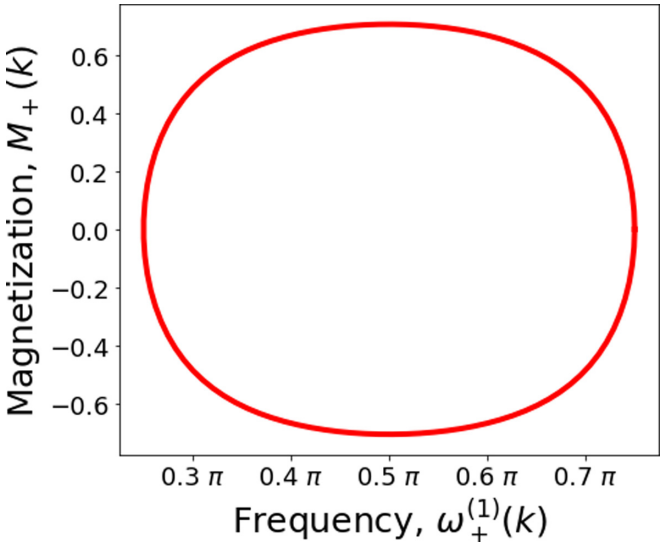

FIG. 3. Typical dependence of $M_+(k)$ from Eq. (24) which forms a symmetric loop around $M = 0$. The x-axis values of the frequency are obtained from Eq. (21). The spectral magnetization $M_s(\omega) = 0$. Here $\theta_1 = \pi/4$ and $\varphi_{1,1} = \varphi_{2,1} = 0$.

$$u_{12}^{(2)} = \sin(\theta_1)\cos(\theta_2)e^{-i(2k-\varphi_{1,2}-\varphi_{2,1})} + \cos(\theta_1)\sin(\theta_2)e^{-i(\varphi_{1,1}-\varphi_{2,2})}. \tag{25}$$

With the help of Eqs. (7) and (8) we obtain the explicit expression for the dispersion relation $\omega_{\pm}^{(2)}(k)$ as

$$\omega_{\pm}^{(2)}(k) = \pm\tfrac{1}{2}\arccos[\cos(\theta_1)\cos(\theta_2)\cos(2k - \varphi_{1,1} - \varphi_{1,2}) - \sin(\theta_1)\sin(\theta_2)\cos(\varphi_{2,1} - \varphi_{2,2})]. \tag{26}$$

Typical band structures are shown in Fig. 4.

In order to possess generalized parity symmetry, Eqs. (18) and (19), it follows from Eq. (25) that $\sin(\theta_1)\sin(\theta_2)\sin(\varphi_{2,2} - \varphi_{2,1}) = 0$. Then it follows that

$$K = \frac{\varphi_{1,1} + \varphi_{1,2}}{2}. \tag{27}$$

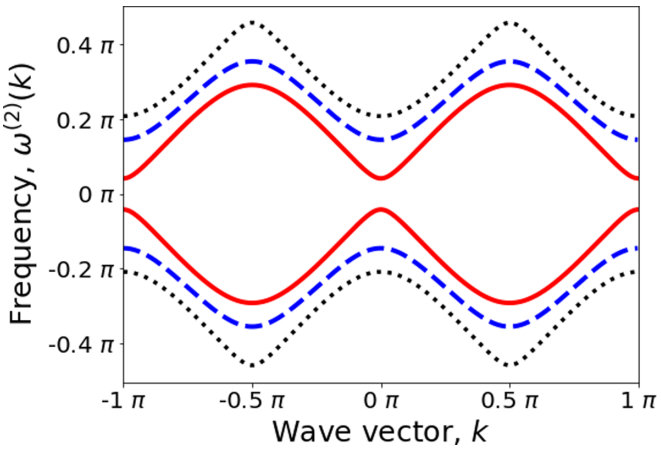

FIG. 4. Dispersion relation $\omega_{\pm}(k)$ for $m = 2$. $\varphi_{2,1} = 0$ (black dotted lines), $\varphi_{2,1} = \pi/2$ (blue dashed line), and $\varphi_{2,1} = \pi$ (red solid line). The other parameters are fixed to $\theta_1 = \pi/4$, $\theta_2 = \pi/6$, and $\varphi_{1,1} = \varphi_{1,2} = \varphi_{2,2} = 0$.

Three symmetry cases can be distinguished:

$$S_{2,1}:\ \theta_1 = n\pi \rightarrow G = 2(\varphi_{2,2} - \varphi_{1,1}), \tag{28}$$

$$S_{2,2}:\ \theta_2 = n\pi \rightarrow G = -2(\varphi_{2,1} + \varphi_{1,1}), \tag{29}$$

$$S_{2,3}:\ \varphi_{2,2} - \varphi_{2,1} = n\pi \rightarrow G = -2(\varphi_{2,1} + \varphi_{1,1}). \tag{30}$$

Here $n = 0, \pm1, \pm2, \ldots$ is an arbitrary integer. If all of the above conditions are broken, then we can expect a nonzero spectral magnetization ratchet to appear. If on the contrary at least one of the above symmetry conditions, $S_{2,1}$, $S_{2,2}$, and $S_{2,3}$, is satisfied, the spectral magnetization vanishes for all frequencies.

For the 2-periodic DTQW the eigenstates are fourfold degenerated, and using Eqs. (25) and (26) we obtain

$$M_+(k) = \frac{\cos(\theta_1)\cos(\theta_2)\sin(2k-2k_0) - \sin(\theta_1)\sin(\theta_2)\sin(\delta\varphi_2)}{|\sin(2\omega_+^{(2)}(k))|}, \tag{31}$$

where $\delta\varphi_2 = \varphi_{2,1} - \varphi_{2,2}$ and $k_0 = (\varphi_{1,1} + \varphi_{1,2})/2$. The typical dependencies of $M_+(k)$ for different values of phase shift $\delta\varphi_2$ are shown in Fig. 5. Nonzero spectral magnetization values appear once $\delta\varphi_2 \neq 0$, signaling the breaking of generalized parity symmetry, Eqs. (28)–(30), and the appearance of the spectral magnetization ratchet.

C. $m = 3$

For the 3-periodic DTQW we calculate the product of the three operators $\hat{U}_1(k)$, $\hat{U}_2(k)$, and $\hat{U}_3(k)$ and get

$$\begin{aligned} u_{11}^{(3)}(k) = {} & \cos(\theta_1)\cos(\theta_2)\cos(\theta_3)e^{i(k_a-3k)} \\ & - \sin(\theta_1)\sin(\theta_2)\cos(\theta_3)e^{i(k_b-k)} \\ & - \sin(\theta_1)\cos(\theta_2)\sin(\theta_3)e^{i(-k_c+k)} \\ & - \cos(\theta_1)\sin(\theta_2)\sin(\theta_3)e^{i(k_d-k)}, \end{aligned} \tag{32}$$

with the notations

$$k_a = \varphi_{1,1} + \varphi_{1,2} + \varphi_{1,3}, \tag{33}$$

$$k_b = \varphi_{1,3} - \varphi_{2,1} + \varphi_{2,2}, \tag{34}$$

$$k_c = \varphi_{1,2} + \varphi_{2,1} - \varphi_{2,3}, \tag{35}$$

$$k_d = \varphi_{1,1} - \varphi_{2,2} + \varphi_{2,3}. \tag{36}$$

Note that $k_a = k_b + k_c + k_d$. The off-diagonal element follows as

$$\begin{aligned} u_{12}^{(3)}(k) = {} & \sin(\theta_1)\cos(\theta_2)\cos(\theta_3)e^{i(k_e-3k)} \\ & + \cos(\theta_1)\sin(\theta_2)\cos(\theta_3)e^{i(k_f-k)} \\ & + \cos(\theta_1)\cos(\theta_2)\sin(\theta_3)e^{i(-k_g+k)} \\ & - \sin(\theta_1)\sin(\theta_2)\sin(\theta_3)e^{i(k_h-k)}, \end{aligned} \tag{37}$$

with the notations

$$k_e = \varphi_{1,2} + \varphi_{1,3} + \varphi_{2,1} = k_a + \varphi_{2,1} - \varphi_{1,1}, \tag{38}$$

$$k_f = -\varphi_{1,1} + \varphi_{1,3} + \varphi_{2,2} = k_b + \varphi_{2,1} - \varphi_{1,1}, \tag{39}$$

$$k_g = \varphi_{1,1} + \varphi_{1,2} - \varphi_{2,3} = k_c - \varphi_{2,1} + \varphi_{1,1}, \tag{40}$$

$$k_h = \varphi_{2,1} - \varphi_{2,2} + \varphi_{2,3} = k_d + \varphi_{2,1} - \varphi_{1,1}. \tag{41}$$

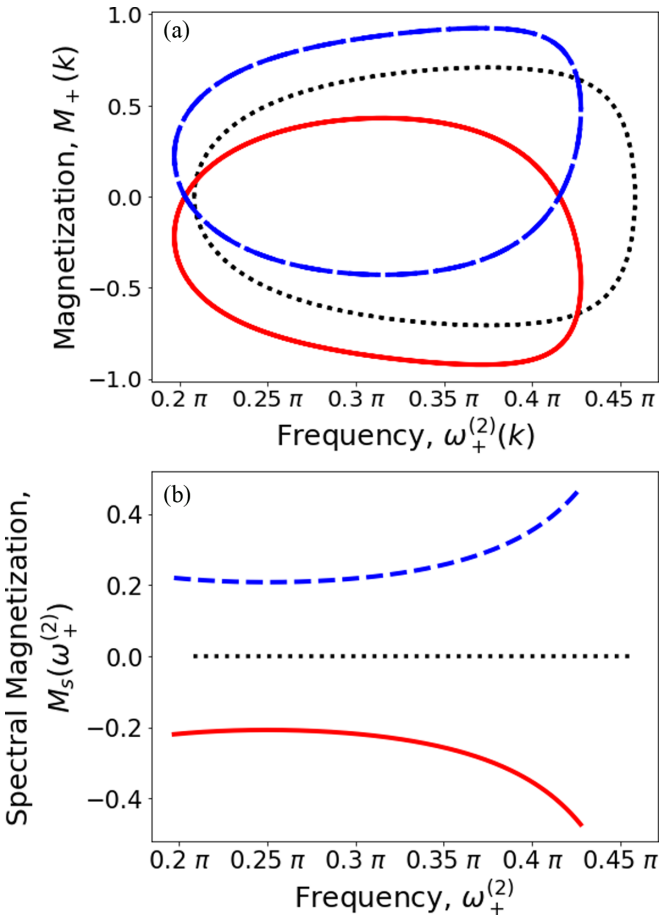

FIG. 5. (a) Typical dependencies of $M_+(k)$ versus $\omega_+^{(2)}(k)$. The black dotted line (symmetric case) $\delta\varphi_2 = 0$; blue dashed line (nonsymmetric case) $\delta\varphi_2 = \pi/5$; red solid line (nonsymmetric case), $\delta\varphi_2 = -\pi/5$. Here $\theta_1 = \pi/4$, $\theta_2 = \pi/6$ and $\varphi_{1,1} = \varphi_{1,2} = 0$. (b) Spectral magnetization $M_s(\omega)$ for the corresponding plots of $M_+(k)$ from panel (a).

Using Eqs. (7) and (8), we obtain the explicit expression for the dispersion relation $\omega_\pm^{(3)}(k)$ as

$$\begin{aligned} \omega_\pm^{(3)}(k) = {} & \pm\tfrac{1}{3}\arccos[\cos(\theta_1)\cos(\theta_2)\cos(\theta_3)\cos(3k - k_a) \\ & - \sin(\theta_1)\sin(\theta_2)\cos(\theta_3)\cos(k - k_b) \\ & - \sin(\theta_1)\cos(\theta_2)\sin(\theta_3)\cos(k - k_c) \\ & - \cos(\theta_1)\sin(\theta_2)\sin(\theta_3)\cos(k - k_d)]. \end{aligned} \tag{42}$$

Typical band structures are shown in Fig. 6.

Let us identify parameters for which the generalized parity symmetry holds. We distinguish two symmetry conditions: $S_{3,1}$ and $S_{3,2}$. $S_{3,1}$ constrains the coin parameters θ_i, while leaving all other angles arbitrary:

$$S_{3,1}:\ \theta_i = n\pi/2, \quad \theta_{j\neq i} = m\pi/2, \tag{43}$$

for arbitrary integers n and m. The details of the cumbersome analysis, including the values of K and G, are given in Appendix A.

The second generalized parity symmetry condition, $S_{3,2}$, constrains all but the coin parameters θ_i. It is realized when $k_a = 3k_b = 3k_c = 3k_d$, which implies $k_b = k_c = k_d$. These

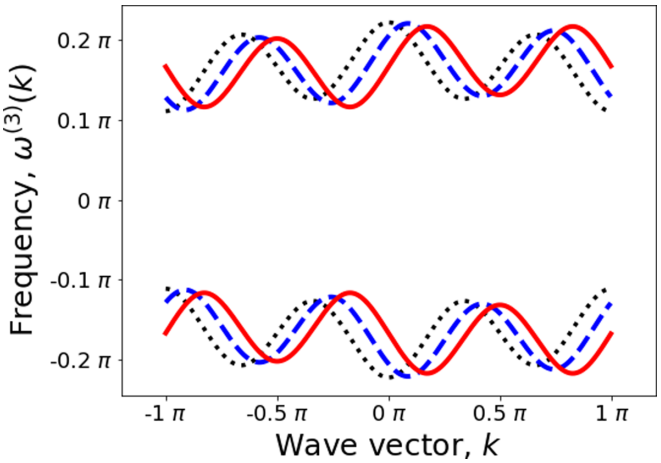

FIG. 6. Dispersion relation $\omega_{\pm}(k)$ for the 3-periodic ($m = 3$) DTQW with different angles $\varphi_{1,1}$: symmetric case $\varphi_{1,1} = 0$ (black dotted line); nonsymmetric cases $\varphi_{1,1} = \pi/4$ (blue dashed line) and $\varphi_{1,1} = \pi/2$ (red solid line). Here $\theta_1 = \pi/3$, $\theta_2 = \pi - 0.43$, and $\theta_3 = 0.43$ are chosen. All other angles are set to zero.

conditions reduce to

$$S_{3,2}\colon \begin{cases} \varphi_{2,2} = \frac{1}{3}(\varphi_{1,1} + \varphi_{1,2} - 2\varphi_{1,3}) + \varphi_{2,1}, \\ \varphi_{2,3} = \frac{1}{3}(-\varphi_{1,1} + 2\varphi_{1,2} - \varphi_{1,3}) + \varphi_{2,1}, \end{cases} \tag{44}$$

with the parameters of the generalized parity symmetry reading:

$$K = k_b, \quad G = 2(\varphi_{2,1} - \varphi_{1,1}). \tag{45}$$

If either of the two symmetries, $S_{3,1}$ or $S_{3,2}$, holds, the spectral magnetization vanishes. If both are violated, a nonzero spectral magnetization ratchet is predicted.

Using Eqs. (32), (42), and (11), we obtain the explicit expression for $M_+(k)$:

$$\begin{aligned} M_+(k) = {} & [\cos(\theta_1)\cos(\theta_2)\cos(\theta_3)\sin(3k - k_a) \\ & - \sin(\theta_1)\sin(\theta_2)\cos(\theta_3)\sin(k - k_b) \\ & + \sin(\theta_1)\cos(\theta_2)\sin(\theta_3)\sin(k - k_c) \\ & - \cos(\theta_1)\sin(\theta_2)\sin(\theta_3)\sin(k - k_d)] \\ & \times \frac{1}{|\sin(3\omega_+^{(3)}(k))|}. \end{aligned} \tag{46}$$

We consider a case where all $\varphi_{i,j} = 0$ except $\varphi_{1,1}$, and $\theta_i \neq n\pi/2$ for any i and any integer n. The corresponding dispersion relation for such a case is shown in Fig. 6. From the previous analysis, it follows that the spectral magnetization must vanish if $\varphi_{1,1} = 0$ since then $S_{3,2}$ is restored. The dependence $M_+(k)$ for different values of the angle $\varphi_{1,1}$ is shown in Fig. 7(a). Indeed the spectral magnetization $M_s(\omega) = 0$ is obtained if $\varphi_{1,1} = 0$ [see black dotted line in Fig. 7(b)], as a direct consequence of the generalized parity symmetry with parameters $K = 0$ and $G = 0$. For nonzero values of $\varphi_{1,1}$, the parity symmetry as described by Eq. (16) is broken, and nonzero values of spectral magnetization are obtained (see blue dashed line and red solid line in Fig. 7).

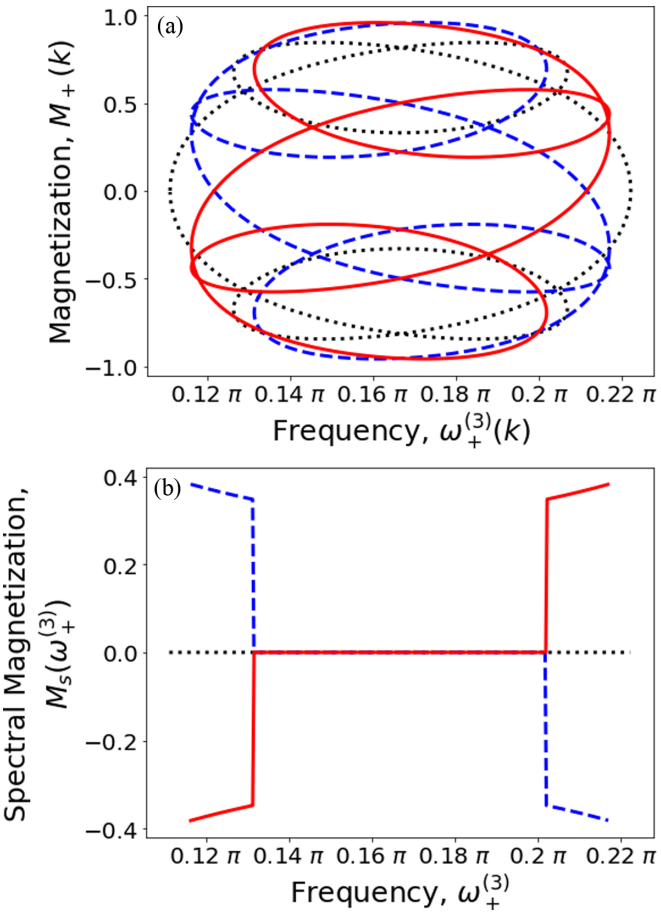

FIG. 7. (a) $M_+^{(3)}(k)$ as a function of frequency $\omega_+^{(3)}(k)$ for different values of $\delta\varphi_{1,1}$: black dotted line (symmetric case), $\varphi_{1,1} = 0$; blue dashed line (nonsymmetric case), $\varphi_{1,1} = \pi/2$; and red solid line (nonsymmetric case), $\varphi_{1,1} = -\pi/2$. Here $\theta_1 = \pi/3$, $\theta_2 = \pi - 0.43$, $\theta_3 = 0.43$, and $\varphi_{1,2} = \varphi_{1,3} = \varphi_{2,1} = \varphi_{2,2} = \varphi_{2,3} = 0$. (b) Spectral magnetization $M_s(\omega)$ for the corresponding plots of $M_+(k)$ in panel (a).

VII. QUANTUM MEASUREMENTS OF THE SPECTRAL MAGNETIZATION RATCHET EFFECT

Let us discuss ways to observe the spectral magnetization $M_s(\omega)$ in the quantum evolution of m-periodic DTQWs. We introduce the time-dependent correlation function

$$\begin{aligned} C_M(t,\tau) = {} & \sum_n \psi_+(n,t)\psi_+^\star(n,t-\tau) \\ & - \psi_-(n,t)\psi_-^\star(n,t-\tau), \end{aligned} \tag{47}$$

where we consider the time steps t and τ as integer multiples of m. Its discrete Fourier-transformation with respect to τ with additional averaging over the discrete time t,

$$C_M(\omega) = \sum_{\tau=0}^{\infty} e^{i\omega\tau}\left[\lim_{T\to\infty}\frac{1}{T}\sum_{t=0}^{T} C_M(t,\tau)\right], \tag{48}$$

can be expressed as

$$C_M(\omega) = \sum_l |\alpha(k_l,\omega)|^2 M(k_l), \tag{49}$$

where the index l in this sum runs over all degenerate points corresponding to the frequency ω. Note here that T is also an integer multiple of m. The coefficients $\alpha(k_l, \omega)$ are determined by the initial conditions:

$$\psi_{\pm}(n, t=0) = \frac{1}{\sqrt{N}} \sum_{k} \sum_{p=\pm} e^{ikn} \alpha(k, \omega_p) \psi_{\pm}(k, \omega_p). \quad (50)$$

Assuming a homogeneous distribution of such coefficients $\alpha(k, \omega)$ such that $|\alpha(k, \omega)|^2 = \text{const}$, we obtain $C_M(\omega) \propto M_s(\omega)$ (see derivation details in Appendix B). Note that the assumption of all basis states having the same weight is similar to a generalized notion of infinite temperature. It follows that the infinite temperature states of quantum Floquet systems like in the case of m-periodic DTQWs may keep a nontrivial internal structure characterized by the presence or absence of certain symmetries.

The correlator $C_M(\omega)$ can be directly measured using a continuous quantum measurement setup proposed and regularly used for the study of quantum dynamics of superconducting qubit networks [40–42]. These setups consist of a low-dissipative transmission line weakly coupled with the studied quantum system (here the DTQW). The transmission line is characterized by a discrete set of internal mode frequencies at which the transmission coefficient is suppressed. Let us consider one such mode with frequency ω_0. Due to the additional coupling of the line with the DTQW the transmission coefficient $D(\omega)$ will display a resonant drop at the resonant frequency ω_{res}:

$$D(\omega) = 1 - \frac{\alpha}{(\omega - \omega_{\text{res}})^2 + \gamma^2}, \quad (51)$$

where α is the strength of the resonance and $\gamma \ll \omega$ is the dissipation parameter. The location of the resonance ω_{res} is renormalized due to the presence of the weakly coupled DTQW: $\omega_{\text{res}} = \omega_0 + \chi C_M(\omega_0)$, where χ is determined by the small coupling strength between the waveguide and the DTQW. Therefore, this method allows one to measure the value of $C_M(\omega)$ and consequently allows one to observe the predicted appearance of the spectral magnetization ratchet.

VIII. CONCLUSION

We have shown that a spectral magnetization ratchet can be observed in a spatially homogeneous DTQW system by breaking a generalized parity symmetry. To achieve that goal, we need to introduce a generalized discrete-time quantum walk process with quantum coins varying periodically in time. As a result, we obtained conditions for the generalized parity symmetry to hold for period $m = 2$ and $m = 3$, and we identified systematic ways to break this symmetry by proper parameter choices. As a result, a nonvanishing spectral magnetization is obtained, which tells that a resonant excitation of all (degenerate) eigenstates at a given eigenfrequency ω will lead to a nonvanishing population imbalance, or simply magnetization. Our results add new possibilities to the control of quantum networks in quantum simulation setups using methods developed in condensed-matter physics.

ACKNOWLEDGMENTS

This work was supported by the Institute for Basic Science, Project Code IBS-R024-D1. P.K. thanks the Center for Theoretical Physics of Complex Systems for hospitality and the Korean Undergraduate Science Program KUSP2019 (kusp.ibs.re.kr) at the Institute for Basic Science for hospitality and financial support. M.V.F. is grateful for the partial financial support of the Ministry of Science and Higher Education of the Russian Federation in the framework of the Increase Competitiveness Program of NUST MISIS K2-2017-081.

APPENDIX A: SYMMETRY $S_{3,1}$ FOR $m = 3$

Here we analyze the generalized parity symmetry $S_{3,1}$ which holds when $\theta_i = n\pi/2$ and $\theta_j = m\pi/2$ are satisfied for any pair of $i \neq j$. In the following n and m are arbitrary integers.

1. $i = 1$ and $j = 2$

(i) For $\theta_1 = (2n+1)\frac{\pi}{2}$ and $\theta_2 = m\pi$, we have

$$u_{11}^{(3)}(k) = -(-1)^{m+n} \sin(\theta_3) e^{i(-k_c+k)},$$
$$u_{12}^{(3)}(k) = (-1)^{m+n} \cos(\theta_3) e^{i(k_e-3k)}$$
$$\Rightarrow u_{11}^{(3)}(2k_c - k) = \left[u_{11}^{(3)}(k)\right]^*,$$
$$u_{12}^{(3)}(2k_c - k) = e^{2i(k_e-3k_c)} \left[u_{12}^{(3)}(k)\right]^*, \quad (A1)$$
$$\Rightarrow K = k_c, \quad G = 2(k_e - 3k_c). \quad (A2)$$

(ii) For $\theta_1 = n\pi$ and $\theta_2 = m\pi$, we have

$$u_{11}^{(3)}(k) = (-1)^{m+n} \cos(\theta_3) e^{i(k_a-3k)},$$
$$u_{12}^{(3)}(k) = (-1)^{m+n} \sin(\theta_3) e^{i(-k_g+k)}$$
$$\Rightarrow u_{11}^{(3)}(2k_a/3 - k) = \left[u_{11}^{(3)}(k)\right]^*,$$
$$u_{12}^{(3)}(2k_a/3 - k) = e^{2ik_a/3-2ik_g} \left[u_{12}^{(3)}(k)\right]^*, \quad (A3)$$
$$\Rightarrow K = k_a/3, \quad G = 2k_a/3 - 2k_g. \quad (A4)$$

(iii) For $\theta_1 = n\pi$ and $\theta_2 = (2m+1)\frac{\pi}{2}$, we have

$$u_{11}^{(3)}(k) = -(-1)^{m+n} \sin(\theta_3) e^{i(k_d-k)},$$
$$u_{12}^{(3)}(k) = (-1)^{m+n} \cos(\theta_3) e^{i(k_f-k)}$$
$$\Rightarrow u_{11}^{(3)}(2k_d - k) = \left[u_{11}^{(3)}(k)\right]^*,$$
$$u_{12}^{(3)}(2k_d - k) = e^{2i(k_f-k_d)} \left[u_{12}^{(3)}(k)\right]^*, \quad (A5)$$
$$\Rightarrow K = k_d, \quad G = 2(k_f - k_d). \quad (A6)$$

(iv) For $\theta_1 = (2n+1)\frac{\pi}{2}$ and $\theta_2 = (2m+1)\frac{\pi}{2}$, we have

$$u_{11}^{(3)}(k) = -(-1)^{m+n} \cos(\theta_3) e^{i(k_b-k)},$$
$$u_{12}^{(3)}(k) = -(-1)^{m+n} \sin(\theta_3) e^{i(k_h-k)},$$
$$\Rightarrow u_{11}^{(3)}(2k_b - k) = \left[u_{11}^{(3)}(k)\right]^*,$$
$$u_{12}^{(3)}(2k_b - k) = e^{2i(k_h-k_b)} \left[u_{12}^{(3)}(k)\right]^*, \quad (A7)$$
$$\Rightarrow K = k_b, \quad G = 2(k_h - k_b). \quad (A8)$$

2. $i = 1$ and $j = 3$

(i) For $\theta_1 = (2n+1)\frac{\pi}{2}$ and $\theta_3 = m\pi$, we have

$$u_{11}^{(3)}(k) = -(-1)^{m+n}\sin(\theta_2)e^{i(k_b-k)},$$
$$u_{12}^{(3)}(k) = (-1)^{m+n}\cos(\theta_2)e^{i(k_e-3k)},$$
$$\Rightarrow u_{11}^{(3)}(2k_b-k) = \left[u_{11}^{(3)}(k)\right]^*,$$
$$u_{12}^{(3)}(2k_b-k) = e^{2i(k_e-3k_b)}\left[u_{12}^{(3)}(k)\right]^* \quad \text{(A9)}$$
$$\Rightarrow K = k_b, \quad G = 2(k_e-3k_b). \quad \text{(A10)}$$

(ii) For $\theta_1 = n\pi$ and $\theta_3 = m\pi$, we have

$$u_{11}^{(3)}(k) = (-1)^{m+n}\cos(\theta_2)e^{i(k_a-3k)},$$
$$u_{12}^{(3)}(k) = (-1)^{m+n}\sin(\theta_2)e^{i(k_f-k)}.$$
$$\Rightarrow u_{11}^{(3)}(2k_a/3-k) = \left[u_{11}^{(3)}(k)\right]^*,$$
$$u_{12}^{(3)}(2k_a/3-k) = e^{2ik_f-2ik_a/3}\left[u_{12}^{(3)}(k)\right]^*, \quad \text{(A11)}$$
$$K = k_a/3, \quad G = 2k_f - 2k_a/3. \quad \text{(A12)}$$

(iii) For $\theta_1 = n\pi$ and $\theta_3 = (2m+1)\frac{\pi}{2}$, we have

$$u_{11}^{(3)}(k) = -(-1)^{m+n}\sin(\theta_2)e^{i(k_d-k)},$$
$$u_{12}^{(3)}(k) = (-1)^{m+n}\cos(\theta_2)e^{i(-k_g+k)},$$
$$\Rightarrow u_{11}^{(3)}(2k_d-k) = \left[u_{11}^{(3)}(k)\right]^*,$$
$$u_{12}^{(3)}(2k_d-k) = e^{-2i(k_g-k_d)}\left[u_{12}^{(3)}(k)\right]^*, \quad \text{(A13)}$$
$$K = k_d, \quad G = -2(k_g-k_d). \quad \text{(A14)}$$

(iv) For $\theta_1 = (2n+1)\frac{\pi}{2}$ and $\theta_3 = (2m+1)\frac{\pi}{2}$, we have

$$u_{11}^{(3)}(k) = -(-1)^{m+n}\cos(\theta_2)e^{i(-k_c+k)},$$
$$u_{12}^{(3)}(k) = -(-1)^{m+n}\sin(\theta_2)e^{i(k_h-k)}$$
$$\Rightarrow u_{11}^{(3)}(2k_c-k) = \left[u_{11}^{(3)}(k)\right]^*,$$
$$u_{12}^{(3)}(2k_c-k) = e^{2i(k_h-k_c)}\left[u_{12}^{(3)}(k)\right]^*, \quad \text{(A15)}$$
$$K = k_c, \quad G = 2(k_h-k_c). \quad \text{(A16)}$$

3. $i = 2$ and $j = 3$

(i) For $\theta_2 = (2n+1)\frac{\pi}{2}$ and $\theta_3 = m\pi$, we have

$$u_{11}^{(3)}(k) = -(-1)^{m+n}\sin(\theta_1)e^{i(k_b-k)},$$
$$u_{12}^{(3)}(k) = (-1)^{m+n}\cos(\theta_1)e^{i(k_f-k)},$$
$$\Rightarrow u_{11}^{(3)}(2k_b-k) = \left[u_{11}^{(3)}(k)\right]^*,$$
$$u_{12}^{(3)}(2k_b-k) = e^{2i(k_f-k_b)}\left[u_{12}^{(3)}(k)\right]^*, \quad \text{(A17)}$$
$$K = k_b, \quad G = 2(k_f-k_b). \quad \text{(A18)}$$

(ii) For $\theta_2 = n\pi$ and $\theta_3 = m\pi$, we have

$$u_{11}^{(3)}(k) = (-1)^{m+n}\cos(\theta_1)e^{i(k_a-3k)},$$
$$u_{12}^{(3)}(k) = (-1)^{m+n}\sin(\theta_1)e^{i(k_e-3k)},$$
$$\Rightarrow u_{11}^{(3)}(2k_a/3-k) = \left[u_{11}^{(3)}(k)\right]^*,$$
$$u_{12}^{(3)}(2k_a/3-k) = e^{2i(k_e-k_a)}\left[u_{12}^{(3)}(k)\right]^*, \quad \text{(A19)}$$
$$K = k_a/3, \quad G = 2(k_e-k_a). \quad \text{(A20)}$$

(iii) For $\theta_2 = n\pi$ and $\theta_3 = (2m+1)\frac{\pi}{2}$, we have

$$u_{11}^{(3)}(k) = -(-1)^{m+n}\sin(\theta_1)e^{i(-k_c+k)},$$
$$u_{12}^{(3)}(k) = (-1)^{m+n}\cos(\theta_1)e^{i(-k_g+k)},$$
$$\Rightarrow u_{11}^{(3)}(2k_c-k) = \left[u_{11}^{(3)}(k)\right]^*,$$
$$u_{12}^{(3)}(2k_c-k) = e^{2i(k_c-k_g)}\left[u_{12}^{(3)}(k)\right]^*, \quad \text{(A21)}$$
$$K = k_c, \quad G = 2(k_c-k_g). \quad \text{(A22)}$$

(iv) For $\theta_2 = (2n+1)\frac{\pi}{2}$ and $\theta_3 = (2m+1)\frac{\pi}{2}$, we have

$$u_{11}^{(3)}(k) = -(-1)^{m+n}\cos(\theta_1)e^{i(k_d-k)},$$
$$u_{12}^{(3)}(k) = -(-1)^{m+n}\sin(\theta_1)e^{i(k_h-k)},$$
$$\Rightarrow u_{11}^{(3)}(2k_d-k) = \left[u_{11}^{(3)}(k)\right]^*,$$
$$u_{11}^{(3)}(2k_d-k) = e^{2i(k_h-k_d)}\left[u_{11}^{(3)}(k)\right]^*, \quad \text{(A23)}$$
$$K = k_d, \quad G = 2(k_h-k_d). \quad \text{(A24)}$$

APPENDIX B: DERIVATION OF THE RELATION BETWEEN THE DISCRETE-TIME-DEPENDENT CORRELATION FUNCTION AND THE SPECTRAL MAGNETIZATION

We consider all time intervals as multiples of m, so that $t, \tau \in m\mathbb{Z}$.

The expectation value of the operator: $(U^{(m)})^{\tau/m}\cdot\hat{M}$ with respect to a general state $|\psi(t)\rangle$ at time step t can be written as

$$\begin{aligned}
&\mathrm{Tr}[|\psi(t)\rangle\langle\psi(t)|\cdot(U^{(m)})^{\tau/m}\cdot\hat{M}]\\
&= \mathrm{Tr}[|\psi(t)\rangle\langle\psi(t-\tau)|\cdot\hat{M}]\\
&= \sum_n\{\langle n|\otimes\langle +|\,|\psi(t)\rangle\langle\psi(t-\tau)|\cdot\hat{M}\,|n\rangle\otimes|+\rangle\}\\
&\quad + \{\langle n|\otimes\langle -|\,|\psi(t)\rangle\langle\psi(t-\tau)|\cdot\hat{M}\,|n\rangle\otimes|-\rangle\}\\
&= \sum_n \psi_+(n,t)\psi_+^*(n,t-\tau) - \psi_-(n,t)\psi_-^*(n,t-\tau).
\end{aligned} \quad \text{(B1)}$$

The last expression in Eq. (B1) is denoted by $C_M(t,\tau)$ in the main text.

We write a general initial state as a superposition of orthogonal basis states (composite states of momentum basis and coin basis):

$$\begin{aligned}
&|\psi(t=0)\rangle\\
&= \sum_k\sum_{p=\pm}\alpha(k,\omega_p(k))\,|k\rangle\otimes|\psi(k,\omega_p(k))\rangle \quad \text{(B2)}\\
&\Rightarrow \psi_\pm(n,t=0) = \langle n,\pm|\psi(t=0)\rangle\\
&= \sum_k\sum_{p=\pm}\langle n|k\rangle\,\alpha(k,\omega_p(k))\psi_\pm(k,\omega_p(k))\\
&= \frac{1}{\sqrt{N}}\sum_k\sum_{p=\pm}e^{ikn}\alpha(k,\omega_p(k))\psi_\pm(k,\omega_p(k)), \quad \text{(B3)}
\end{aligned}$$

with N being the number of lattice sites, so that

$$|k\rangle = \frac{1}{\sqrt{N}} \sum_n e^{ikn} |n\rangle \Rightarrow \langle n|k\rangle = \frac{1}{\sqrt{N}} e^{ikn}. \tag{B4}$$

The general state at any time step t is

$$\psi_\pm(n,t) = \frac{1}{\sqrt{N}} \sum_{k,p} e^{ikn - i\omega_p(k)t} \alpha(k, \omega_p(k)) \psi_\pm(k, \omega_p(k)). \tag{B5}$$

Therefore,

$$\begin{aligned}
&\psi_+(n,t)\psi_+^*(n,t-\tau) \\
&= \frac{1}{N} \sum_{k,p} \sum_{k',p'} e^{i(k-k')n} e^{-i\omega_p(k)t} \alpha(k, \omega_p(k)) \psi_+(k, \omega_p(k)) \\
&\quad \times e^{i\omega_{p'}(k')(t-\tau)} \alpha^*(k', \omega_{p'}(k')) \psi_+^*(k', \omega_{p'}(k')).
\end{aligned} \tag{B6}$$

Using $\sum_{n=1}^N e^{i(k-k')n} = N\delta_{kk'}$, we get

$$\begin{aligned}
&\sum_n \psi_+(n,t)\psi_+^*(n,t-\tau) \\
&= \sum_k \left[\sum_p e^{-i\omega_p(k)t} \alpha(k, \omega_p(k)) \psi_+(k, \omega_p(k)) \right] \\
&\quad \times \left[\sum_{p'} e^{i\omega_{p'}(k)(t-\tau)} \alpha^*(k, \omega_{p'}(k)) \psi_+^*(k, \omega_{p'}(k)) \right] \\
&= \sum_k \sum_p e^{-i\omega_p(k)\tau} |\alpha(k, \omega_p(k))|^2 |\psi_+(k, \omega_p(k))|^2 \\
&\quad + \sum_k \sum_{p \neq p'} e^{-i\omega_p(k)t} \alpha(k, \omega_p(k)) \psi_+(k, \omega_p(k)) \\
&\quad \times e^{i\omega_{p'}(k)(t-\tau)} \alpha^*(k, \omega_{p'}(k)) \psi_+^*(k, \omega_{p'}(k)).
\end{aligned} \tag{B7}$$

Averaging over the time steps t leads to a vanishing of the cross terms in Eq. (B7) since

$$\lim_{T\to\infty} \frac{1}{T} \sum_{t=0}^T e^{\pm i[\omega_-(k) - \omega_+(k)]t} = \delta_{\omega_+(k)\,\omega_-(k)} = 0, \tag{B8}$$

where T is also an integer multiple of m. Therefore we arrive at

$$\begin{aligned}
C_M(\tau) &= \lim_{T\to\infty} \frac{1}{T} \sum_{t=0}^T C_M(t,\tau) \\
&= \sum_k \sum_{p=\pm} e^{-i\omega_p(k)\tau} |\alpha(k, \omega_p(k))|^2 |\psi_+(k, \omega_p(k))|^2 \\
&\quad - e^{-i\omega_p(k)\tau} |\alpha(k, \omega_p(k))|^2 |\psi_-(k, \omega_p(k))|^2.
\end{aligned} \tag{B9}$$

Applying a discrete Fourier transform from the time domain τ to the frequency domain ω, we arrive at

$$\begin{aligned}
C_M(\omega) &= \lim_{T\to\infty} \frac{1}{T} \sum_{\tau=0}^T e^{i\omega\tau} C_M(\tau) \\
&= \sum_l |\alpha(k_l, \omega)|^2 |\psi_+(k_l, \omega)|^2 - |\alpha(k_l, \omega)|^2 |\psi_-(k_l, \omega)|^2 \\
&= \sum_l |\alpha(k_l, \omega)|^2 M(k_l).
\end{aligned} \tag{B10}$$

In Eq. (B10) the last sum runs over all such k_l which yield the same frequency ω. If the initial state was a superposition of all basis states with coefficients whose absolute values are equal, such that

$$|\alpha(k, \omega_+(k))| = |\alpha(k, \omega_-(k))| = \frac{1}{\sqrt{2N}} \text{ for all } k, \tag{B11}$$

we finally obtain

$$C_M(\omega) = \frac{1}{2N} M_s(\omega). \tag{B12}$$

Note that the assumption of all basis states having the same weight is similar to a generalized notion of infinite temperature. In other words $C_M(\tau)$ will be the expectation value of the operator $(U^{(m)})^{\tau/m} \cdot \hat{M}$ with respect to the density matrix $\rho = \frac{1}{2N} \sum_k \sum_p |k\rangle \langle k| \otimes |\psi(k, \omega_p(k))\rangle \langle \psi(k, \omega_p(k))|$. The density matrix ρ is diagonal in eigenbasis of the evolution operator $U^{(m)}$, the eigenstates probabilities are equal, and hence it describes a thermal state at infinite temperature. The proposed measurement is therefore expected to be capable of detecting a symmetry breaking in the evolution of a quantum Floquet system.

[1] P. Reimann, Brownian motors: Noisy transport far from equilibrium, Phys. Rep. **361**, 57 (2002).

[2] F. Julicher, A. Ajdari, and J. Prost, Modeling molecular motors, Rev. Mod. Phys. **69**, 1269 (1997).

[3] P. Hanggi, F. Marchesoni, and F. Nori, Brownian motors, Ann. Phys. **14**, 51 (2005).

[4] S. Denisov, S. Flach, and P. Hanggi, Tunable transport with broken space-time symmetries, Phys. Rep. **538**, 77 (2014).

[5] S. Flach, O. Yevtushenko, and Y. Zolotaryuk, Directed Current due to Broken Time-Space Symmetry, Phys. Rev. Lett. **84**, 2358 (2000).

[6] S. Flach, Y. Zolotaryuk, A. E. Miroshnichenko, and M. V. Fistul, Broken Symmetries and Directed Collective Energy Transport in Spatially Extended Systems, Phys. Rev. Lett. **88**, 184101 (2002).

[7] G. Carapella and G. Costabile, Ratchet Effect: Demonstration of a Relativistic Fluxon Diode, Phys. Rev. Lett. **87**, 077002 (2001).

[8] C. Zhang, C.-F. Li, and G.-C. Guo, Experimental demonstration of photonic quantum ratchet, Sci. Bull. **60**, 249 (2015).

[9] P. Reimann, M. Grifoni, and P. Hanggi, Quantum Ratchets, Phys. Rev. Lett. **79**, 10 (1997).

[10] S. Denisov, L. Morales-Molina, and S. Flach, Quantum resonances and rectification in ac-driven ratchets, Europhys. Lett. **79**, 10007 (2007).

[11] S. Denisov, L. Morales-Molina, S. Flach, and P. Hanggi, Periodically driven quantum ratchets: Symmetries and resonances, Phys. Rev. A **75**, 063424 (2007).

[12] J. B. Majer, J. Peguiron, M. Grifoni, M. Tusveld, and J. E. Mooij, Quantum Ratchet Effect for Vortices, Phys. Rev. Lett. **90**, 056802 (2003).

[13] T. Salger, S. Kling, T. Hecking, C. Geckeler, L. M. Molina, and M. Weitz, Directed transport of atoms in a Hamiltonian quantum ratchet, Science **326**, 1241 (2009).

[14] C. Drexler, S. A. Tarasenko, P. Olbrich, J. Karch, M. Hirmer, F. Muller, M. Gmitra, J. Fabian, R. Yakimova, S. Lara-Avila *et al.*, Magnetic quantum ratchet effect in graphene, Nat. Nanotechnol. **8**, 104 (2013).

[15] S. Flach and A. A. Ovchinnikov, Static magnetization induced by time-periodic fields with zero mean, Phys. A (Amsterdam, Neth.) **292**, 268 (2001).

[16] S. Flach, A. E. Miroshnichenko, and A. A. Ovchinnikov, ac-driven quantum spins: Resonant enhancement of transverse dc magnetization, Phys. Rev. B **65**, 104438 (2002).

[17] Y. Aharonov, L. Davidovich, and N. Zagury, Quantum random walks, Phys. Rev. A **48**, 1687 (1993).

[18] N. B. Lovett, S. Cooper, M. Everitt, M. Trevers, and V. Kendon, Universal quantum computation using the discrete-time quantum walk, Phys. Rev. A **81**, 042330 (2010).

[19] S. Singh, P. Chawla, A. Sarkar, and C. M. Chandrashekar, Computational power of single qubit discrete-time quantum walk, arXiv:1907.04084.

[20] I. Vakulchyk, M. V. Fistul, P. Qin, and S. Flach, Anderson localization in generalized discrete-time quantum walks, Phys. Rev. B **96**, 144204 (2017).

[21] A. Crespi, R. Osellame, R. Ramponi, V. Giovannetti, R. Fazio, L. Sansoni, F. D. Nicola, F. Sciarrino, and P. Matalon, Anderson localization of entangled photons in an integrated quantum walk, Nat. Photon. **7**, 322 (2013).

[22] I. Vakulchyk, M. V. Fistul, and S. Flach, Wave Packet Spreading with Disordered Nonlinear Discrete-Time Quantum Walks, Phys. Rev. Lett. **122**, 040501 (2019).

[23] T. Kitagawa, M. S. Rudner, E. Berg, and E. Demler, Exploring topological phases with quantum walks, Phys. Rev. A **82**, 033429 (2010).

[24] J. K. Asboth, Symmetries, topological phases, and bound states in the one-dimensional quantum walk, Phys. Rev. B **86**, 195414 (2012).

[25] T. Rakovszky and J. K. Asboth, Localization, delocalization, and topological phase transitions in the one-dimensional split-step quantum walk, Phys. Rev. A **92**, 052311 (2015).

[26] S. Panahiyan and S. Fritzsche, Simulation of the multiphase configuration and phase transitions with quantum walks utilizing a step-dependent coin, Phys. Rev. A **100**, 062115 (2019).

[27] M. Maeda, H. Sasaki, E. Segawa, A. Suzuki, and K. Suzuki, Dynamics of solitons for nonlinear quantum walks, J. Phys. Commun. **3**, 075002 (2019).

[28] A. Mallick and C. M. Chandrashekar, Dirac cellular automaton from split-step quantum walk, Sci. Rep. **6**, 25779 (2016).

[29] A. Mallick, S. Mandal, A. Karan, and C. M. Chandrashekar, Simulating Dirac Hamiltonian in curved space-time by split-step quantum walk, J. Phys. Commun. **3**, 015012 (2019).

[30] P. Arnault, A. Pérez, P. Arrighi, and T. Farrelly, Discrete-time quantum walks as fermions of lattice gauge theory, Phys. Rev. A **99**, 032110 (2019).

[31] J. Du, H. Li, X. Xu, M. Shi, J. Wu, X. Zhou, and R. Han, Experimental implementation of the quantum random-walk algorithm, Phys. Rev. A **67**, 042316 (2003).

[32] T. Di, M. Hillery, and M. S. Zubairy, Cavity QED-based quantum walk, Phys. Rev. A **70**, 032304 (2004).

[33] D. A. Meyer, Noisy quantum Parrondo games, in *Fluctuations and Noise in Photonics and Quantum Optics*, edited by D. Abbott, J. H. Shapiro, and Y. Yamamoto (SPIE, Bellingham, Washington, 2003), Vol. 5111, pp. 344–350.

[34] S. Chakraborty, A. Das, A. Mallick, and C. M. Chandrashekar, Quantum ratchet in disordered quantum walk, Ann. Phys. **529**, 1600346 (2017).

[35] J. Rajendran and C. Benjamin, Playing a true Parrondo's game with a three-state coin on a quantum walk, Europhys. Lett. **122**, 40004 (2018).

[36] P. Ribeiro, P. Milman, and R. Mosseri, Aperiodic Quantum Random Walks, Phys. Rev. Lett. **93**, 190503 (2004).

[37] G. D. Molfetta, M. Brachet, and F. Debbasch, Quantum walks in artificial electric and gravitational fields, Phys. A (Amsterdam, Neth.) **397**, 157 (2014).

[38] C. Cedzich and R. F. Werner, Revivals in quantum walks with a quasiperiodically-time-dependent coin, Phys. Rev. A **93**, 032329 (2016).

[39] N. P. Kumar, R. Balu, R. Laflamme, and C. M. Chandrashekar, Bounds on the dynamics of periodic quantum walks and emergence of the gapless and gapped Dirac equation, Phys. Rev. A **97**, 012116 (2018).

[40] A. Wallraff, D. I. Schuster, A. Blais, L. Frunzio, R. S. Huang, J. Majer, S. Kumar, S. M. Girvin, and R. J. Schoelkopf, Strong coupling of a single photon to a superconducting qubit using circuit quantum electrodynamics, Nature (London) **431**, 162 (2004).

[41] P. A. Volkov and M. V. Fistul, Collective quantum coherent oscillations in a globally coupled array of superconducting qubits, Phys. Rev. B **89**, 054507 (2014).

[42] P. Macha, G. Oelsner, J. M. Reiner, M. Marthaler, S. Andre, G. Schon, U. Hubner, H. G. Meyer, E. Il'ichev, and A. V. Ustinov, Implementation of a quantum metamaterial using superconducting qubits, Nat. Commun. **5**, 5146 (2014).